

Lasers in Manufacturing Conference 2013

Formation dynamics of ultra-short laser induced micro-dots in the bulk of transparent materials

A. Mermillod-Blondin^{a*}, D. Ashkenasi^b, A. Lemke^b, M. Schwagmeier^b,
A. Rosenfeld^a

^aMax-Born-Institut für Nichtlineare Optik und Kurzzeitspektroskopie, Max-Born-Straße 2a, 12489 Berlin, Germany

^bLaser- und Medizin-Technologie GmbH, Fabekstr. 60-62, 14195 Berlin, Germany

Abstract

In this paper, we study the formation dynamics of ultra-short laser-induced micro dots under the surface of transparent materials. Laser-induced micro dots find their application in direct part marking, to address full life cycle traceability. We first demonstrate the possibility of direct laser part marking into the cladding of an optical fiber. Then, we monitor the laser affected zone with the help of a time-resolved phase contrast microscopy setup in a fused silica substrate. We show that the transient energy relaxation processes affect the host material over a region that exceeds the micro dot size by several micrometers.

© 2013 The Authors. Published by Elsevier B.V. Open access under [CC BY-NC-ND license](https://creativecommons.org/licenses/by-nc-nd/4.0/).
Selection and/or peer-review under responsibility of the German Scientific Laser Society (WLT e.V.)

Keywords: ultra-short laser processing, direct part marking and machining, micro dots, time-resolved microscopy

1. Motivation

Laser marking is among the best available technologies employed for direct part marking, a key process in the quest of “cradle-to-grave” product traceability. At the present time, direct part marking is always performed onto the surface of the device that has to be identified. Obviously, surface marking presents the risk that the integrity of the marking may be jeopardized through any possible surface damage (scratch, wear

* Corresponding author. Tel.: +49-30-63921214; Fax: +49-30-63921299.
E-mail address: mermillod@mbi-berlin.de

etc.). Therefore, embedded marking (i.e. direct part marking under the surface) would offer a higher grade of security whenever transparent parts are under consideration. Thanks to their high peak intensities, ultra-short laser pulses stand out as a unique tool for micro processing the bulk of transparent materials with a high precision [1]. Indeed, the processed volume is limited to the region where the laser energy is sufficiently high to trigger multi-photon absorption. By playing on basic parameters such as the focusing strength or the laser pulse energy, micro sized dots (micro dots) can be imprinted into the bulk of any transparent solid. Micro dots correspond to localized laser-induced structural modifications translating into a refractive index change (Δn). Whether Δn is positive, negative, or both mostly depends on the chemical composition of the host material and on the laser intensity. It was also demonstrated that the temporal shape of the laser excitation pulse can dictate the sign of Δn [2]. This flexibility reinforces the potential of ultra-short lasers for marking applications.

Another driving application is placing micro dots into a quartz glass fiber [3]. The possibility of inducing micro modifications acting as scattering centers inside the wave guide without removing the buffer or even the jacket stimulates the growing interest of industrial implementation. The intention is the fabrication of so-called diffusers near the distal end of a medical wave guide. These diffusers can be used for medical therapy, e.g. laser interstitial thermo therapy (LITT). One major obstacle is the introduction of a sufficient density of micro dots inside the core to receive a collective side scattering rate of greater 90% along a pre-defined length (e.g. 20 mm) without reducing the necessary stability of the ultra-short laser processed wave guide. Hence, means of controlling the character of the micro dots, density changes and the size of a stress field related to changes in Δn , is of great importance.

Fig. 1 depicts examples of laser induced micro dots inside a 400 μm quartz wave guide placed near the core-cladding interface, similar to the work published in Ref. 3, only using a picosecond laser source. Note that the micro dots imaged from the side demonstrate a cylindrical elongation in direction of the laser pulses generating the modifications. The aspect ratio of these micro dots can be adjusted somewhat by varying the laser parameters, such as pulse energy. However, there is a strong strive of searching for other strategies in controlling size and nature of the laser induced micro modifications. A better understanding on the reaction mechanisms inside the bulk of transparent material after ultra-short laser pulse excitation is necessary to develop processing strategies for future implementations and to demonstrate that ultra-short bulk machining does not affect the functionality of the new device. In order to do so, we developed a time-resolved phase contrast microscopy apparatus. Our experimental results provide insights into the dynamics of laser energy relaxation. We monitor the evolution of the laser-affected zone in the vicinity of the focal volume with a nanosecond time-resolution.

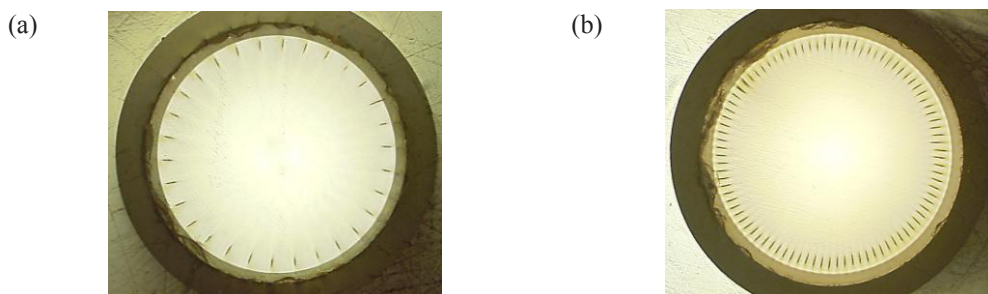


Fig. 1. Microscope images of the exit surface of a quartz wave guide with embedded micro dots in the 400 μm core (close to the cladding interface): (a) ca. 30 individual lines of micro dots, (b) ca. 80 individual lines of micro dots.

2. Experimental

The time-resolved phase contrast microscope is shown in Fig. 2. Our setup is based on a commercially available phase contrast microscope integrated into a pump-probe scheme. We replaced the initial light bulb illumination by a pulsed YAG laser (probe) synchronized with the femtosecond laser source (pump). In this configuration, we are able to monitor the real part of the laser-induced refractive index with a temporal resolution of 1 ns. The beam profile of the YAG laser is homogenized by a pair of diffusers. As a consequence, the illumination background exhibits a speckled aspect. We mounted the second diffuser on a rotating motor moving continuously. By accumulating 50 pictures, each picture corresponding to a new diffuser position, the speckle contrast drops by a factor of ~ 7 [4]. The femtosecond laser source delivers 150 fs (full width at half maximum) light pulses with a spectrum centered around 800 nm. The nominal repetition rate of 166 Hz is scaled down to 3 Hz by an external electromechanical shutter (not shown in Fig. 2). The focusing objective has a numerical aperture of 0.45. The fused silica sample, a $3 \times 20 \times 20 \text{ mm}^3$ parallelepiped, is mounted on X,Y,Z motorized translation stages (not represented in Fig. 2). During the acquisition, the sample is continuously scanned so that each femtosecond laser pulse interacts with a pristine material. A positive phase contrast microscope objective forms an image of the laser irradiated volume on the surface of an electron multiplying CCD detector. A bandpass filter placed in front of the detector (532 nm central wavelength, 25 nm width) minimizes the contribution of laser-induced plasma emission to the final image.

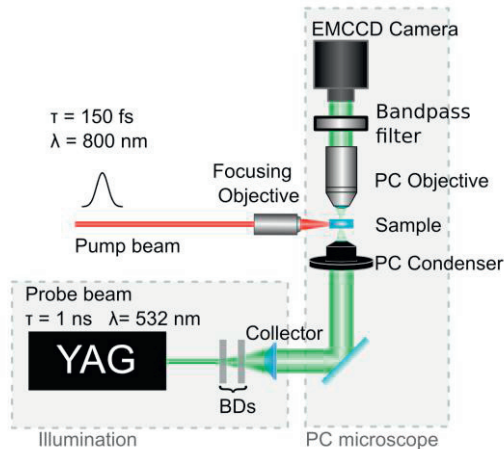


Fig. 2. Time-resolved phase contrast microscopy setup. BDs: beam diffusers, PC: phase contrast, EMCCD: electron multiplying charge coupled device. The bandpass filter is centered around 532 nm with a total bandwidth of 25 nm.

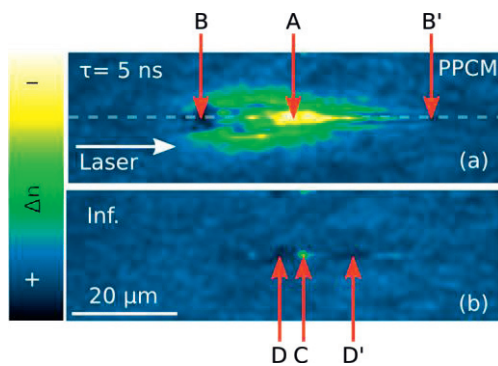


Fig. 3. (a) Time-resolved phase contrast microscopy picture taken 5 ns after the fs laser excitation. (b). Phase contrast picture taken in the same illumination as (a), in permanent regime, i.e. several milliseconds after the fs laser excitation. Dotted line: optical axis. PPCM: positive phase contrast microscopy. Irradiation conditions: one single pulse, $4 \mu\text{J}$

3. Results and Discussion

In Fig. 3, we compare the morphology of the irradiated region 5 ns after the laser excitation and in permanent regime, several milliseconds after the femtosecond laser excitation in positive phase contrast microscopy (PPCM). In PPCM, pixels darker than the background denote an increase of the real part of the refractive index whereas pixels lighter than the background correspond to a decrease of the refractive index. The laser pulse energy was 4 μJ . The fs laser pulse propagates from left to right. The plane of observation corresponds to the plane of incidence.

For the clarity of the discussion, we divide Fig. 3a in regions A, B and B'. Phase contrast microscopy reveals that region A has a refractive index smaller than the non-irradiated material. The possible laser-induced effects producing a transient refractive index decrease are mainly point defects and local stress related to the thermoelastic response of the irradiated material. Under the conjugated effect of strong focusing and nonlinear propagation, the energy deposition into the bulk material is strongly inhomogeneous, resulting in the onset of a "hot spot" in region A. One important consequence of high energy exposure is the generation of a dense free electron plasma. Given that permanent material damage occurs, a transient electron density n_e close to the critical density ($n_c = 1.74 \cdot 10^{21} \text{ cm}^{-3}$) at the end of the laser pulse is realistic. Although the free electron self-trapping dynamics take place with a time constant of about 150 fs, self-trapped excitons (STEs) relax into point defect structures surviving at least on the nanosecond timescale. In particular, STEs can decay into E' centers with energy levels close to the conduction band. According to the Lorentz model, such point defects bring a negative contribution to the local refractive index [5]. At a time of 5 ns after excitation, thermoelastic transformations also start to play a role. The electron bath and the ionic cores have reached an equilibrium temperature, as thermalization takes place on the picosecond timescale. The heated volume tends to expand and leaves behind a material rarefied zone, which agrees well with a refractive index decrease in region A. This expanding region compresses the surrounding material (hoop stress). Material compaction tends to be stronger where the lattice is already softened, resulting in regions of higher refractive index B and B'.

Figure 3b shows the aspect of the laser-induced micro dot when the energy relaxation is over. Again, we define three regions (labeled C, D and D'). Region C corresponds to a microsphere of about 1.5 μm radius exhibiting a negative refractive index change. Previous experimental results [6] suggest that this voidlike object is a result of thermal expansion beyond the plastic limit. The material structure inside region C is still unclear. Interestingly, a similar laser-induced voidlike structure appears upon fs laser irradiation in GeO_2 [7]. Based on Raman spectroscopy measurements, the authors established that this voidlike structure contains mostly molecular O_2 . Regions D and D' have a higher refractive index, indicating that the laser-induced structural changes taking place are different. A positive refractive index change is consistent with a local alteration of the network structure following moderately high laser exposure. More specifically, Chan et al. [8] have reported an experimental proof of laser-induced densification of amorphous fused silica through a localized alteration of the material Qn structure.

4. Conclusion

The mechanisms responsible for a transient refractive index change on the nanosecond timescale are mostly related to laser induced stress and thermal flow. The laser-induced stress is generated through the thermo-elastic response of the material following plasma relaxation. The plasma relaxation can also result in the onset of point defects with consequences on the local refractive index.

Time-resolved phase contrast microscopy investigations clearly demonstrate that the laser-affected zone is more extended than the remaining micro dot. In consequence, we advise letting a free space of at least 10 μm

around the modified region to guarantee sub-surface marking and processing applications with minimal damage and long-term stability.

Acknowledgements

Part of this study is supported by an AiF/IGF program “Generierung spannungsarmer Innenmarkierungen (micro-dots)“, project number 16891 BG (20/8).

References

- [1] R. Gattass, E. Mazur, *Laser micromachining in transparent materials*, Nat. Photonics 2, p. 219-225; 2008.
- [2] A.Mermillod-Blondin, I.M. Burakov, Y.P. Meshcheryakov, N.M. Bulgakova, E. Audouard, A. Rosenfeld, A. Husakou, I.V. Hertel, R. Stoian, *Flipping the sign of refractive index changes in ultrafast and temporally shaped laser-irradiated borosilicate crown optical glass at high repetition rates*, Phys. Rev. B 77, 104205; 2008.
- [3] A. Lemke, D. Ashkenasi, T. Trebst, H.J. Eichler, *Ultra-short laser pulse processing of non-stripped medical quartz fiber wave guides*, Proceedings of the Fifth International WLT-Conference on Lasers in Manufacturing, 479-482; 2009.
- [4] J.W. Goodman, *Speckle phenomena in optics*; 2007.
- [5] S. Mao, F. Quéré, S. Guizard, X. Mao, R. Russo, G. Petite, P. Martin, *Dynamics of femtosecond laser interactions with dielectrics*, Appl. Phys. A: Mater. Sci. Process. 79, 1695-1709; 2004.
- [6] A. Mermillod-Blondin, J. Bonse, A. Rosenfeld, I.V. Hertel, Y.P. Meshcheryakov, N.M. Bulgakova, E. Audouard, R. Stoian, *Dynamics of femtosecond laser induced voidlike structures in fused silica*, Appl. Phys. Lett., 94, 041911; 2009.
- [7] L. Bressel, D. de Ligny, E.G. Gamaly, A.V. Rode, S. Juodkazis, *Observation of O₂ inside voids formed in GeO₂ glass by tightly-focused fs-laser pulses*, Opt. Mater. Express 1, 1150-1157; 2011.
- [8] J.W. Chan, T. Huser, S. Risbud, D.M. Krol, *Structural changes in fused silica after exposure to focused femtosecond laser pulses*, Opt. Lett.; 26, 1726-1728; 2001.